American Mineralogist, Volume 104, pages 1851–1856, 2019

Bicapite, $KNa_2Mg_2(H_2PV^{5+}_{14}O_{42})\cdot 25H_2O$, a new polyoxometalate mineral with a bicapped Keggin anion from the Pickett Corral mine, Montrose County, Colorado, U.S.A.

ANTHONY R. KAMPF[1,*], JOHN M. HUGHES[2], BARBARA P. NASH[3], AND JOE MARTY[4]

[1]Mineral Sciences Department, Natural History Museum of Los Angeles County, 900 Exposition Boulevard, Los Angeles, California 90007, U.S.A.
[2]Department of Geology, University of Vermont, Burlington, Vermont 05405, U.S.A.
[3]Department of Geology and Geophysics, University of Utah, Salt Lake City, Utah 84112, U.S.A.
[4]5199 East Silver Oak Road, Salt Lake City, Utah 84108, U.S.A.

ABSTRACT

Bicapite, $KNa_2Mg_2(H_2PV^{5+}_{14}O_{42})\cdot 25H_2O$, is a new mineral species (IMA2018-048) discovered at the Pickett Corral mine, Montrose County, Colorado, U.S.A. Bicapite occurs as square tablets up to about 0.2 mm on edge on montroseite-corvusite-bearing sandstone. Crystals are dark red-brown, often appearing black. The streak is orange, and the luster is vitreous. Bicapite is brittle, has a Mohs hardness of 1½, and displays one excellent cleavage on {100}. The measured density is 2.44(2) g/cm^3. Bicapite is uniaxial (+), $\omega = 1.785(5)$, $\varepsilon \approx 1.81$ (white light); pleochroism is red-brown; $E > O$, slight. The electron probe microanalysis and results of the crystal structure determination provided the empirical formula (based on 67 O apfu) $(K_{1.23}Na_{2.23}Mg_{1.48})_{\Sigma 4.94}[H_{2.51}P_{1.02}(V^{5+}_{13.91}Mo^{6+}_{0.07})_{\Sigma 13.98}O_{42}]\cdot 25H_2O$. Bicapite is tetragonal, $I4/m$, with $a = 11.5446(12)$ Å, $c = 20.5460(14)$ Å, $V = 2738.3(6)$ Å^3, and $Z = 2$. The strongest four lines in the diffraction pattern are [d in Å (I) (hkl)]: 10.14 (100) (002,101); 2.978 (29) (134,206); 2.809 (11) (305); and 2.583 (11) (420,008). The atomic arrangement of bicapite was solved and refined to $R_1 = 0.0465$ for 1008 independent reflections with $I > 2\sigma I$. The structural unit is a $[H_2PV^{5+}_{12}O_{40}(V^{5+}O)_2]^{7-}$ heteropolyanion composed of 12 distorted VO_6 octahedra surrounding a central PO_4 tetrahedron and capped on opposite sides by two VO_5 square pyramids; the structural unit is a modification of the α-isomer of the Keggin anion, $[XM_{12}O_{40}]^{n-}$. Charge balance in the structure is maintained by the $[KNa_2Mg_2(H_2O)_{25}]^{7+}$ interstitial complex. The name bicapite is in recognition of this being the only known mineral with a structure based on a bicapped Keggin anion. The discovery of bicapite and numerous other natural polyoxometalate compounds in the Colorado Plateau uranium/vanadium deposits make that the most productive region found to date for naturally occurring polyoxometalate compounds.

Keywords: Bicapite, new mineral, crystal structure, polyoxometalate, bicapped Keggin anion, Pickett Corral mine, Montrose County, Colorado, U.S.A.

INTRODUCTION

The arcuate 120 km long Uravan Mineral Belt of the Colorado Plateau has been a rich source of uranium and vanadium ores since early in the twentieth century. The numerous mines in the belt exploit roll-front deposits in the sandstone of the Salt Wash member of the Morrison Formation (Carter and Guiltieri 1965; Shawe 2011). The mineralization of U and V took place where solutions rich in U^{6+}- and V^{4+}/V^{5+}-bearing aqueous species encountered local strongly reducing conditions, typically due to the presence of organic matter. The geochemistry of the deposits and conditions of deposition were first examined in detail by Evans and Garrels (1958). The uranium and vanadium deposits of the Uravan Mineral Belt have also been a rich source of new minerals; more than 30 minerals with essential vanadium have been discovered there since 2008 during collecting undertaken by one of the authors (J.M.) and his colleagues. These minerals have added extensively to the knowledge of the complexity of naturally occurring vanadium compounds.

The new mineral bicapite was found underground in the Pickett Corral mine, Bull Canyon, Montrose County, Colorado, about 13 km west of the town of Naturita. The portal to the Pickett Corral mine is located at 38.195272, –108.843326; however, the partially flooded workings of the mine were accessed through the main portal of the interconnected Blue Streak mine located at 38.199434, –108.839946. The Pickett Corral mine is in the central portion of the Uravan Mineral Belt. The new mineral forms from the oxidation of montroseite-corvusite assemblages in a moist environment. Under ambient temperatures and generally oxidizing near-surface conditions, water reacts with pyrite to form aqueous solutions with relatively low pH; this water reacts with unoxidized and oxidized phases that have been exposed by mining operations to form bicapite and other new mineral species.

The name bicapite is in recognition of this being the only known mineral with a structure based on a bicapped Keggin anion. The mineral was collected on March 24, 2016, by one of the authors (J.M.), Al Wilkins, and Okie Howell. It has been found very sparingly on only several small specimens. It occurs on montroseite-corvusite-bearing sandstone in close association with gypsum, huemulite, and thenardite. Bicapite was approved by the Commission on New Minerals, Nomenclature and Classification of the International Mineralogical Association (IMA 2018-048).

---

[*] E-mail: akampf@nhm.org

0003-004X/19/0012–1851$05.00/DOI: https://doi.org/10.2138/am-2019-7027

Two co-type specimens of bicapite are deposited in the collections of the Natural History Museum of Los Angeles County, Los Angeles, California, U.S.A., catalog numbers 66915 and 66916.

POLYOXOMETATES

Polyoxometalate compounds (often abbreviated as POMs) are relatively rare in geology, but of great importance in synthetic chemistry and materials science. Polyoxometalates, usually anionic in nature, are clusters of three or more transition metal-centered polyhedra that are linked by sharing oxygen ligands between and among the polyhedra. The linked polyhedra form a three-dimensional framework. One example of a polyoxometalate compound recently found to be common to numerous minerals in the Colorado Plateau deposits is the $[V_{10}O_{28}]^{6-}$ isopolyanion, the decavanadate group, formed of 10 VO_6 octahedra linked through corner- and edge-sharing. Typically, bonding within the polyoxometalate is stronger than between the polyoxometalate and the surrounding crystal field.

Polyoxometalates are important phases in industrial chemistry, where a large effort is expended in synthesizing polyoxometalates with desirable characteristics of size, charge, shape, and conformation. Many hundreds of papers are published annually in the chemistry literature on polyoxometalates, and the number of papers has been increasing logarithmically since the early 1990s (Hutin et al. 2013); a similar increase in patents involving polyoxometalates is also noted (Katsoulis 1998). In a detailed survey of industrial uses of polyoxometalates, Katsoulis (1998) notes that 80–85% of the patents issued for polyoxometalates are in the area of catalysis, with the remaining 15–20% involving the compounds in nearly a score of other applications, including coatings, sorbents of gases, sensors, dyes, capacitors, cation exchangers, anti-tumor agents, and bleaching of pulp paper. New uses of polyoxometalate compounds have been in medicine as antiviral agents, cancer antagonists, and treatment for Alzheimer's disease, and in nanomagnetism with applications to semiconductors and quantum computing.

There are many methods of synthesis of polyoxometalates, but the most common method is undertaken using acidic aqueous systems that contain the relevant polyoxometalate cations and the cations needed to balance the charge of the anionic polyoxometalate at a controlled pH; molybdate and tungstate polyoxometalates tend to occur at lower pH values than vanadate POMs. The conditions of vanadium polyoxometalate formation in laboratory aqueous synthesis are similar to the natural post-mining conditions found in the Colorado plateau vanadium-uranium mines, where solutions rich in vanadium for the POM formation as well as charge-balancing cations exist at a suitable pH.

Although polyoxometalate compounds are not common in minerals, they do exist, and a growing number of POMS are being discovered in the Colorado Plateau Uravan Belt; these phases are listed subsequently. In addition to those minerals with a similar Colorado Plateau genesis to bicapite, POM-bearing minerals include zunyite (Baur and Ohta 1982) and murataite (Ercit and Hawthorne 1995); however, in these minerals, the Keggin-type polyoxometalates are condensed into frameworks and do not contain independent polyoxometalate units. The Colorado Plateau deposits have enlarged the number of POM-bearing minerals greatly, and that region is the most productive region found to date for naturally occurring polyoxometalate compounds.

APPEARANCE, OPTICAL AND PHYSICAL PROPERTIES

Bicapite occurs as square tablets up to about 0.2 mm on edge (Figs. 1 and 2); the crystals are dark red brown, often appearing black. The streak is orange, and the luster is vitreous. Bicapite is non-fluorescent under long- and short-wave ultraviolet light. It is brittle, has a Mohs hardness of 1½ (based upon scratch tests), and exhibits excellent cleavage on {100}; the fracture is irregular, stepped. The density measured by flotation in methylene iodide–toluene is 2.44(2) g/cm^3; the calculated density is 2.434 g/cm^3 for the empirical formula and 2.428 g/cm^3 for the ideal formula. Bicapite is very slowly soluble in room-temperature H_2O (~1 h); the phase decomposes in dilute HCl at room temperature and then slowly dissolves.

Optical observations on bicapite were made in white light. Bicapite is uniaxial (+), with $\omega = 1.785(5)$ and $\varepsilon \approx 1.81$. Note that ε is observed to be slightly greater than 1.80; in liquids >1.80, crystals of an unknown phase immediately grow on the surfaces of the bicapite crystals. Pleochroism is red-brown; $E > O$, slight. The Gladstone-Dale compatibility (Mandarino 2007), $1 - (K_p/K_c)$, is –0.017 (superior) using the empirical formula and –0.019 (superior) using the ideal formula.

CHEMICAL COMPOSITION

Analyses of bicapite (4 points on 3 crystals) were performed at the University of Utah on a Cameca SX-50 electron microprobe with four wavelength-dispersive spectrometers, and utilizing Probe for EPMA software. Analytical conditions were 15 keV

FIGURE 1. Bicapite with huemulite (orange) and minor gypsum; FOV 0.48 mm across.

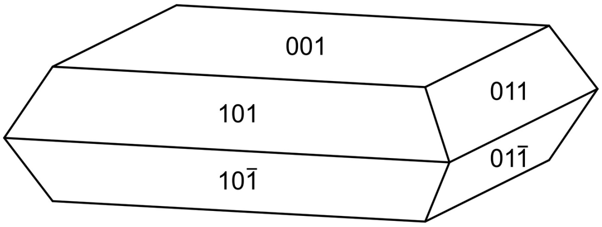

FIGURE 2. Crystal drawing of bicapite; clinographic projection.

accelerating voltage, 10 nA beam current, and a beam diameter of 5 to 10 μm. Counting times were 20 s on peak and 20 s on background for each element. Raw X-ray intensities were corrected for matrix effects with a ϕρ(z) algorithm (Pouchou and Pichoir 1991). A time-dependent correction was applied to the data for Na to allow for an intensity decrease during analysis. All other elements exhibited no time-dependence in intensity.

No damage from the electron beam was observed. However, as is typical of highly hydrated phases with weakly held H_2O, bicapite partially dehydrates under vacuum either during carbon coating or in the microprobe chamber. This results in an irregular surface for analysis. In addition, the H_2O loss results in higher concentrations for the remaining constituents than are to be expected for the fully hydrated phase. Because an insufficient quantity of bicapite is available for a direct determination of H_2O, that content has been calculated based upon the structure determination. Elemental concentrations are given in Table 1.

The empirical formula (based on 42 O apfu in structural unit) is $(K_{1.23}Na_{2.23}Mg_{1.48})_{\Sigma 4.94}[H_{2.51}P_{1.02}(V^{5+}_{13.91}Mo^{6+}_{0.07})_{\Sigma 13.98}O_{42}]\cdot 25H_2O$. The simplified formula is $KNa_2Mg_2(H_2PV^{5+}_{14}O_{42})\cdot 25H_2O$, which corresponds to K_2O 2.35, Na_2O 3.10, MgO 4.03, P_2O_5 3.54, V_2O_5 63.59, H_2O 23.39, total 100 wt%.

CRYSTAL-STRUCTURE DETERMINATION

Powder X-ray diffraction was performed using a Rigaku R-Axis Rapid II curved imaging plate microdiffractometer with monochromatized Mo$K\alpha$ radiation. A Gandolfi-like motion on the φ and ω axes was used to randomize the samples. Observed *d* values and intensities were derived by profile fitting using JADE 2010 software. Data, including unit-cell parameters refined from the powder data using JADE 2010 with whole pattern fitting, are given in Supplemental[1] Table S1.

Single-crystal X-ray studies were carried out using the same instrument and radiation noted above. The Rigaku CrystalClear software package was used for processing the structure data, including the application of numerical and empirical absorption corrections, the latter with the multi-scan approach using ABSCOR (Higashi 2001). The structure was solved by direct methods using SIR2011 (Burla et al. 2012). SHELXL-2016 (Sheldrick 2015) was used for the refinement of the structure. The occupancies of the interstitial cation sites were refined, with the K site refined with full joint occupancy by K and O (H_2O). A residual peak 2.229(17) Å from the K site was refined as an additional low-occupancy H_2O site; however, based upon distances to surrounding O sites, it could also accommodate additional Na. All non-hydrogen sites were refined with anisotropic displacement parameters. Difference Fourier syntheses located all H atom positions, except those associated with the partially occupied H_2O sites and those that protonate the bicapped Keggin anion. The H sites were refined with soft restraints of 0.82(3) Å on the O–H distances and 1.30(3) Å on the H–H distances; the U_{eq} of each H was set to 1.2 times that of the donor O atom. Data collection and refinement details are given in Table 2, atom coordinates and displacement parameters in Table 3, selected bond distances in Table 4, and bond-valence sums in Table 5.

TABLE 1. Compositional data (wt%) for bicapite

Const.	Mean	Range	S.D.	Standard	Norm.
K_2O	3.49	3.32–3.65	0.17	sanidine	2.89
Na_2O	4.16	3.68–4.52	0.35	albite	3.44
MgO	3.59	3.45–3.80	0.16	diopside	2.97
P_2O_5	4.35	4.15–4.49	0.15	apatite	3.60
V_2O_5	76.25	75.72–76.69	0.54	V metal	63.04
MoO_3	0.61	0.42–0.77	0.18	Mo metal	0.50
H_2O*					23.57
Total					100.01

* Based upon the crystal structure with V + P + Mo = 15 and O = 67 apfu.

ATOMIC ARRANGEMENT OF BICAPITE

The atomic arrangement of bicapite (Figs. 3 and 4) consists of two distinct parts, a structural unit and an interstitial complex, as suggested by Schindler and Hawthorne (2000) for such hydrated minerals with a polyanion. The structural unit is a $[H_2PV^{5+}_{12}O_{40}(V^{5+}O)_2]^{7-}$ heteropolyanion composed of 12 distorted VO_6 octahedra surrounding a central PO_4 tetrahedron and capped on opposite sides by two VO_5 square pyramids, which share four of their edges with VO_6 octahedra (Fig. 3). Without the two capping tetrahedra (and H atoms of the structural unit), the heteropolyanion is the α-isomer of the Keggin anion, $[XM_{12}O_{40}]^{n-}$, which in this case has the formula $[PV^{5+}_{12}O_{40}]^{15-}$. In light of the bond valence sum (BVS) values for the V sites all being slightly greater than 5 v.u., all V in the mineral is likely to be in the +5 oxidation state. The central PO_4 tetrahedron is disordered, with eight half-occupied O atoms around the P. This is consistent with the P residing at the 0, 0, ½ special position with 4/*m* symmetry. Attempts to refine the structure in a space group that would allow P to occupy a site with $\overline{4}$ symmetry were unsuccessful. It should be noted that this same sort of averaged orientation of the central Keggin tetrahedron has been reported in other structures (cf. Nyman et al. 2007).

The interstitial complex includes two octahedrally coordinated cation sites, one occupied by Mg and surrounded by six H_2O groups and one occupied by Na and surrounded by five H_2O groups and one O atom. The $Mg(H_2O)_6$ octahedron is isolated and only links to other structural components via hydrogen bonding.

TABLE 2. Data collection and structure refinement details for bicapite

Diffractometer	Rigaku R-Axis Rapid II
X-ray radiation/power	Mo$K\alpha$ (λ = 0.71075 Å)/50 kV, 40 mA
Temperature	293(2) K
Empirical formula	$H_{42}K_{1.49}Mg_{1.89}Na_{1.93}O_{66.98}P_1V_{14}$
Space group	*I*4/*m*
Unit-cell dimensions	a = 11.5446(12) Å c = 20.5460(14) Å
V	2738.3(6) Å^3
Z	2
Density (for above formula)	2.434 g/cm^3
Absorption coefficient	2.594 mm^{-1}
F(000)	1974.1
Crystal size	140 × 80 × 30 μm
θ range	3.19 to 24.98°
Index ranges	$-13 \le h \le 12$, $-13 \le k \le 13$, $-24 \le l \le 24$
Refls collected/unique	10217/1245; R_{int} = 0.057
Reflections with $I > 2\sigma I$	1008
Completeness to θ = 24.98°	99.4%
Max. and min. transmission	0.926 and 0.713
Refinement method	Full-matrix least-squares on F^2
Parameters/restraints	141/10
GoF	1.100
Final *R* indices [$F_o > 4\sigma(F)$]	R_1 = 0.0465, wR_2 = 0.1133
R indices (all data)	R_1 = 0.0578, wR_2 = 0.1214
Largest diff. peak/hole	+0.54/–0.60 e/A^3

*$R_{int} = \Sigma|F_o^2 - F_o^2(\text{mean})|/\Sigma[F_o^2]$. GoF = $S = \{\Sigma[w(F_o^2 - F_c^2)^2]/(n-p)\}^{1/2}$. $R_1 = \Sigma||F_o| - |F_c||/\Sigma|F_o|$. $wR_2 = \{\Sigma[w(F_o^2 - F_c^2)^2]/\Sigma[w(F_o^2)^2]\}^{1/2}$; $w = 1/[\sigma^2(F_o^2) + (aP)^2 + bP]$ where *a* is 0.0578, *b* is 13.824, and *P* is $[2F_c^2 + \text{Max}(F_o^2,0)]/3$.

TABLE 3. Atom coordinates and displacement parameters (Å^2) for bicapite

	x/a	*y/b*	*z/c*	U_{eq}	Occupancy
P	0	0	0.5	0.0201(7)	1
V1	0	0	0.31386(8)	0.0295(4)	1
V2	0.29689(10)	–0.05685(10)	0.5	0.0306(4)	1
V3	0.18565(7)	0.12493(7)	0.38618(4)	0.0313(3)	1
Mg	0.5	0	0.25	0.0305(13)	0.944(15)
Na	0.5	0.5	0.62235(19)	0.0415(17)	0.966(17)
K/O	0.3951(3)	0.2637(3)	0.5	0.0608(17)	K: 0.372(14); O: 0.628(14)
OW	0.4463(12)	0.1529(14)	0.5841(8)	0.025(6)	0.184(11)
O1	0.1059(5)	–0.0230(5)	0.4572(3)	0.0264(14)	0.5
O2	0	0	0.2361(3)	0.0416(18)	1
O3	0.2624(3)	0.1777(3)	0.32880(17)	0.0412(9)	1
O4	0.4277(4)	–0.0938(4)	0.5	0.0469(14)	1
O5	0.0299(3)	0.1487(3)	0.34411(19)	0.0393(9)	1
O6	0.2960(5)	0.0526(3)	0.4346(2)	0.0711(15)	1
O7	0.1688(3)	0.2447(5)	0.4368(2)	0.0792(18)	1
OW1	0.5	0.500000	0.5	0.060(3)	1
H1	0.52(2)	0.569(7)	0.5	0.071	1
OW2	0.5	0	0.3506(3)	0.0447(13)	1
H2	0.543(4)	–0.021(6)	0.378(2)	0.054	1
OW3	0.4516(3)	0.1778(3)	0.2505(2)	0.0428(10)	1
H3A	0.385(3)	0.186(5)	0.265(3)	0.051	1
H3B	0.456(5)	0.229(4)	0.223(2)	0.051	1
OW4	0.5446(5)	0.2936(5)	0.6219(3)	0.0746(15)	1
H4A	0.602(5)	0.270(7)	0.605(3)	0.090	1
H4B	0.550(7)	0.275(7)	0.6599(16)	0.090	1

	U^{11}	U^{22}	U^{33}	U^{23}	U^{13}	U^{12}
P	0.0213(10)	0.0213(10)	0.0176(16)	0	0	0
V1	0.0349(6)	0.0349(6)	0.0186(8)	0	0	0
V2	0.0254(6)	0.0316(7)	0.0349(7)	0	0	–0.0006(4)
V3	0.0329(5)	0.0386(5)	0.0223(5)	–0.0006(3)	0.0037(3)	–0.0078(3)
Mg	0.0341(16)	0.0341(16)	0.023(2)	0	0	0
Na	0.050(2)	0.050(2)	0.024(3)	0	0	0
K	0.047(2)	0.063(3)	0.073(3)	0	0	0.0022(16)
OW	0.012(9)	0.036(11)	0.027(10)	–0.006(7)	–0.009(7)	–0.005(6)
O1	0.032(3)	0.030(3)	0.018(3)	–0.003(3)	0.003(3)	0.002(3)
O2	0.052(3)	0.052(3)	0.020(4)	0	0	0
O3	0.039(2)	0.054(2)	0.031(2)	0.0046(17)	0.0069(16)	–0.0083(17)
O4	0.027(3)	0.038(3)	0.076(4)	0	0	–0.001(2)
O5	0.0282(18)	0.041(2)	0.049(2)	–0.0127(17)	–0.0020(16)	0.0022(14)
O6	0.116(4)	0.033(2)	0.064(3)	0.016(2)	–0.059(3)	–0.021(2)
O7	0.035(2)	0.130(4)	0.073(3)	–0.070(3)	–0.014(2)	0.025(2)
OW1	0.069(5)	0.069(5)	0.040(7)	0	0	0
OW2	0.046(3)	0.061(4)	0.028(3)	0	0	0.000(3)
OW3	0.040(2)	0.044(2)	0.044(2)	0.0035(18)	0.0128(18)	0.0039(17)
OW4	0.079(4)	0.059(3)	0.086(4)	0.001(3)	0.023(3)	0.015(3)

TABLE 4. Selected bond distances (Å) and angles (°) in bicapite

P-O1 (×4)	1.529(6)	**V3-O3**	**1.596(3)**	Na-O2	2.338(8)
		V3-O7	**1.742(4)**	Na-OW4 (×4)	2.438(5)
V1-O2	**1.597(7)**	V3-O6	1.818(4)	Na-OW1	2.514(4)
V1-O5 (×4)	1.858(3)	V3-O5	2.014(3)	<Na-O>	2.434
<V1-O>	1.858	V3-O5	2.031(3)		
		V3-O1	2.388(6)	K-O4	2.833(6)
V2-O4	**1.569(5)**	<V3-O>	1.999	K-O7 (×2)	2.925(5)
V2-O6 (×2)	1.845(4)			K-OW1	2.985(4)
V2-O7 (×2)	1.928(4)	Mg-OW2 (×2)	2.068(5)	K-O6 (×2)	3.009(5)
V2-O1	2.405(6)	Mg-OW3 (×4)	2.128(4)	K-OW4 (×2)	3.061(6)
<V2-O>	1.990	<Mg-O>	2.116	<K-O>	2.976

Hydrogen bonds

D–H···*A*	*D*–H	H···*A*	*D*···*A*	Δ*D*–H–*A*
OW1-H1···K(H_2O)	0.84(3)	2.16(6)	2.985(4)	166(7)
OW2-H2···O6	0.79(3)	2.22(3)	2.982(7)	162(6)
OW3-H3a···O3	0.83(3)	1.93(3)	2.712(5)	157(5)
OW3-H3b···O5	0.82(3)	1.98(3)	2.800(6)	178(6)
OW4-H4a···O7	0.80(3)	2.28(3)	3.074(8)	169(8)
OW4-H4b···OW3	0.81(3)	2.44(5)	3.131(8)	144(8)

Note: V-O vanadyl bonds (Schindler and Hawthorne 2000) in bold.

The $NaO(H_2O)_5$ octahedra form dimers by linking through one shared H_2O group. Each end of the dimer is an O atom shared with the apical O atoms of the VO_5 square pyramids that cap different bicapped Keggin anions. Above the four square "cavities" in each bicapped Keggin anion is the site jointly occupied by K and H_2O. When the site is occupied by K, it forms bonds to the four O atoms at the corners of the cavity, one bond to an O atom in a different bicapped Keggin anion and three bonds to H_2O groups belonging to the $NaO(H_2O)_5$ octahedra. When the K site is occupied by the O atom of an H_2O group, it presumably forms hydrogen bonds to surrounding O atoms. One such bond is probably to O4, thereby compensating for its otherwise low BVS (1.86 v.u.).

The interstitial complex ideally has the formula $[KNa_2Mg_2(H_2O)_{25}]^{7+}$, which, for charge balance, requires that the structural unit is doubly protonated. Although no specific H sites could be identified on the periphery of the bicapped Keggin anion, among synthetic bicapped Keggin anions, protonation is quite common. For example, Kato et al. (1982) described a similar bicapped Keggin anion for which they gave the formula $H_nPV_{14}O_{42}^{(9-n)-}$. In bicapite, the most likely candidate O sites for partial OH character are probably O2, O3, and O4, because of their somewhat low BVS values and their locations on the periphery of the structural unit, although as noted above, the low BVS for O4 may be compensated by a hydrogen bond from the H_2O group partially occupying the K site. The low BVS for the PO_4 group O1 site (1.69 v.u.) is probably due to steric effects rather than being indicative of partial OH character. For comparison, the O atom of the PO_4 group in the similar bicapped Keggin anion reported by Kato et al. (1982) is 1.74 v.u. corresponding to a P–O bond length of 1.529 Å (identical to the P–O distance in bicapite).

A note on bonding within the structural unit and between the structural unit and the interstitial complex is in order. The exterior oxygen atoms of the heteropolyanionic structural unit that protrude into the interstitial unit (O2, O3, O4), known as "terminal" O atoms, are all bound to the vanadium atoms of the structural unit by vanadyl bonds (Table 4; Schindler et al. 2000), as is a fourth oxygen atom (O7) that is an also an exterior atom but not a terminal oxygen. Three of these four oxygen atoms are shared with atoms of the interstitial complex (Na-O2, K-O4, K-O7). In addition, O6, although not bonded to vanadium with a vanadyl bond, is bound to two vanadium atoms in addition to the interstitial, partially occupied, K site. The strongly anisodesmic nature of bonding in the polyanionic structural group is illustrated by the bond valence (in valence units, v.u.) each of its oxygen atoms receives from the cations of the polyanion: O1 = 1.69; O2 = 1.68; O3 = 1.69; O4 = 1.81; O5 = 1.98; O6 = 1.84; O7 = 1.88). Such bonding has implications for the solution behavior of the polyanions and ion transport in the ore-forming fluids of the Colorado Plateau.

IMPLICATIONS

Over the past several years, numerous new minerals have been described from the mines of the Colorado Plateau. In addition to the previously described Colorado Plateau mineral sherwoodite (Evans and Konnert 1978) and numerous new $[V_{10}O_{28}]^{6-}$ decavanadate minerals (Kampf et al. 2017a), there is a growing number of recently described Colorado-Plateau minerals with large, complex heteropolyanions. The minerals vanarsite, packratite, morrisonite, and gatewayite all contain

TABLE 5. Bond-valence sums for bicapite

	K	Na	Mg	P	V1	V2	V3	H bonds		Σ
								Acc.	Don.	
O1				1.27 (×4↓)		0.21	0.22 (×½↓→), 0.20 (×½↓→)			1.69
O2		0.22			1.68					1.90
O3							1.69	0.22		1.91
O4	0.14 (×0.37→)					1.81				1.86
O5					0.86 (×4↓)		0.57, 0.55	0.18		2.16
O6	0.09 (×2↓) (×0.37→)					0.89 (×2↓)	0.95	0.13		2.00
O7	0.11 (×2↓) (×0.37→)					0.72 (×2↓)	1.16	0.12		2.04
OW1	0.10 (×4 ×0.37→)	0.14 (×2→)							–0.11,–0.11	0.06
OW2			0.35 (×2↓)						–0.13,–0.13	0.09
OW3			0.31 (×4↓)					0.11	–0.22,–0.18	0.01
OW4	0.08 (×2↓) (×0.37→)	0.17 (×4↓)							–0.11	0.09
Σ	0.80	1.04	1.94	5.08	5.12	5.23	5.13			

Notes: Values are expressed in valence units. Bond valence parameters are from Gagné and Hawthorne (2015); hydrogen-bond strengths based on O-O bond lengths are from Ferraris and Ivaldi (1988).

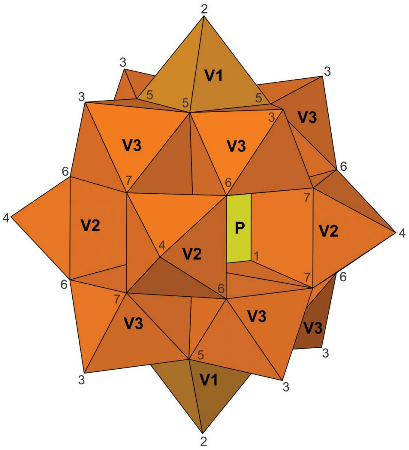

FIGURE 3. Bicapped Keggin anion that is the $[H_2PV^{5+}_{12}O_{40}(V^{5+}O)_2]^{7-}$ structural unit in bicapite. The O atom sites are numbered. The **c** axis is approximately vertical.

the $[As^{3+}As^{5+}_6V^{4+}_{2+x}V^{5+}_{10-x}O_{51}]^{(11+x)-}$ heteropolyanion, a novel polyoxometalate cluster (Kampf et al. 2016). The mineral kegginite (Kampf et al. 2017b) contains the $[As^{5+}V^{5+}_{12}O_{40}(VO)]^{12-}$ monocapped ε-isomer of the Keggin heteropolyanion, and ophirite contains a heteropolytungstate tri-lacunary Keggin anion $[Fe^{3+}W_9O_{34})_2]^{11-}$ (Kampf et al. 2014). Herein we describe bicapite, a mineral whose structure contains the $[H_2PV^{5+}_{12}O_{40}(V^{5+}O)_2]^{7-}$ protonated bicapped α-isomer of the Keggin heteropolyanion. Other new minerals of the region that contain large heteropolyions, both anionic and cationic, are currently under study. The mines of the Colorado Plateau are a rich source of minerals with complex heteropolyions that have formed in low-temperature, post-mining mineral assemblages, apparently similar to the "one-pot" bench-scale synthesis of polyoxometalates in inorganic chemistry (Hutin et al. 2013), and obviously forming in a self-assembling environment. The discovery and study of those self-organizing nanostructures advance our knowledge and understanding of mineral complexity on Earth, provide new insights into complex ions that can exist in near-surface environments, and inform researchers in other fields of new avenues to explore in developing phases with potential technological uses. The Colorado Plateau uranium/vanadium deposits encompass the most productive region found to date for naturally occurring polyoxometalate compounds.

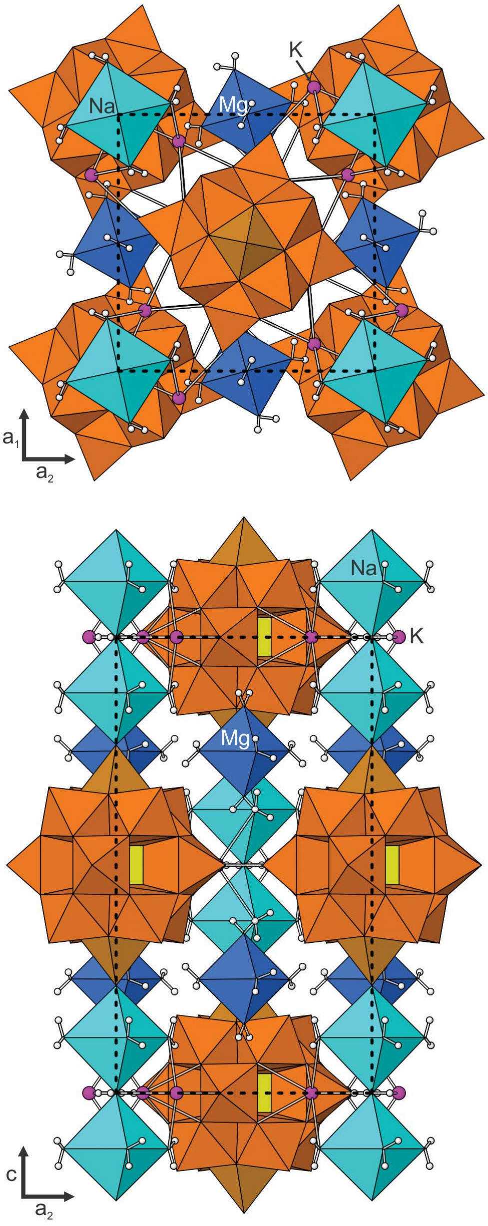

FIGURE 4. Structure of bicapite viewed down **c** (top) and **a** (bottom). H atoms are shown as white balls. The unit cell is outlined with dashed lines.

ACKNOWLEDGMENTS

The manuscript was improved by reviews by Michael Schindler and an anonymous review. Editorial handling by Fernando Colombo is greatly appreciated.

FUNDING

This study was funded, in part, by the John Jago Trelawney Endowment to the Mineral Sciences Department of the Natural History Museum of Los Angeles County and by grant NSF-MRI 1039436 from the National Science Foundation to J.M.H. B.P.N. thanks the Northern California Mineralogical Association for partial support for electron microprobe analyses of new minerals from the Colorado Plateau.

REFERENCES CITED

Baur, W.H., and Ohta, T. (1982) The Si_5O_{16} pentamer in zunyite refined and empirical relations for individual silicon-oxygen bonds. Acta Crystallographica, B38, 390–401.

Burla, M.C., Caliandro, R., Camalli, M., Carrozzini, B., Cascarano, G.L., Giacovazzo, C., Mallamo, M., Mazzone, A., Polidori, G., and Spagna, R. (2012) SIR2011: a new package for crystal structure determination and refinement. Journal of Applied Crystallography, 45, 357–361.

Carter, W.D., and Gualtieri, J.L. (1965) Geology and uranium–vanadium deposits of the La Sal quadrangle, San Juan County, Utah, and Montrose County, Colorado. U.S. Geological Survey Professional Paper 508.

Ercit, T.S., and Hawthorne, F.C. (1995) Murataite, a UB_{12} derivative structure with condensed Keggin molecules. Canadian Mineralogist, 33, 1223–1229.

Evans, H.T. Jr., and Garrels, R.M. (1958) Thermodynamic equilibria of vanadium in aqueous systems as applied to the interpretation of the Colorado Plateau ore deposits. Geochimica et Cosmochimica Acta, 15, 131–149.

Evans, H.T. Jr., and Konnert, J.A. (1978) The crystal chemistry of sherwoodite, a calcium 14-vanadoaluminate heteropoly complex. American Mineralogist, 63, 863–868.

Ferraris, G., and Ivaldi, G. (1988) Bond valence vs. bond length in O···O hydrogen bonds. Acta Crystallographica, B44, 341–344.

Gagné, O.C., and Hawthorne, F.C. (2015) Comprehensive derivation of bond-valence parameters for ion pairs involving oxygen. Acta Crystallographica, B71, 562–578.

Higashi, T. (2001) ABSCOR. Rigaku Corporation, Tokyo.

Hutin, M., Rosnes, M.H., Long, D.-L., and Cronin, L. (2013) Polyoxometalates: Synthesis and structure—From building blocks to emergent structures. In J. Reedijk and K. Poeppelmeier, Eds., Comprehensive Inorganic Chemistry II, 2, p. 241–269. Elsevier.

Kampf, A.R., Hughes, J.M., Nash, B.P., Wright, S.E., Rossman, G.R., and Marty, J. (2014) Ophirite, $Ca_2Mg_4[Zn_2Mn_2^{3+}(H_2O)_2(Fe^{3+}W_9O_{34})_2]\cdot 46H_2O$, a new mineral with a heteropolytungstate tri-lacunary Keggin anion. American Mineralogist, 99, 1045–1051.

Kampf, A.R., Hughes, J.M., Nash, B.P., and Marty, J. (2016) Vanarsite, packratite, morrisonite, and gatewayite: four new minerals containing the $[As^{3+}V_{12}^{4+,5+}As_6^{5+}O_{51}]$ heteropolyanion, a novel polyoxometalate cluster. Canadian Mineralogist, 54, 145–162.

Kampf, A.R., Nash, B.P., Marty, J., Hughes, J.M., and Rose, T.P. (2017a) Hydropascoite, $Ca_3(V_{10}O_{28})\cdot 24H_2O$, a new decavanadate mineral from the Packrat mine, Mesa County, Colorado. Canadian Mineralogist, 55, 207–217.

Kampf, A.R., Hughes, J.M., Nash, B.P., and Marty, J. (2017b) Kegginite, $Pb_3Ca_3[AsV_{12}O_{40}(VO)]\cdot 20H_2O$, a new mineral with an ε-isomer of the Keggin anion. American Mineralogist, 102, 461–465.

Kato, R., Kobayashi, A., and Sasaki, Y. (1982) The heteropolyvanadate of phosphorus. Crystallographic and NMR Studies. Inorganic Chemistry, 21, 240–246.

Katsoulis, D. (1998) A survey of applications of polyoxometalates. Chemistry of Materials, 98, 359–387.

Mandarino, J.A. (2007) The Gladstone–Dale compatibility of minerals and its use in selecting mineral species for further study. Canadian Mineralogist, 45, 1307–1324.

Nyman, M., Maginn, E.J., Larentzos, J.P., Bonhomme, F.J., Parise, B., Welk, M.E., Bull, I., and Park, H. (2007) Experimental and theoretical methods to investigate extraframework species in a layered material of dodecaniobate anions. Inorganic Chemistry, 46, 2067–2079.

Pouchou, J.-L., and Pichoir, F. (1991) Quantitative analysis of homogeneous or stratified microvolumes applying the model "PAP." In K.F.J. Heinrich and D.E. Newbury, Eds., Electron Probe Quantitation, p. 3l–75. Plenum Press.

Schindler, M., and Hawthorne, F.C. (2000) A bond-valence approach to the structure, chemistry, and paragenesis of hydroxyl-hydrated oxysalt minerals. I. Theory. Canadian Mineralogist, 39, 1225–1242.

Schindler, M., Hawthorne, F.C., and Baur, W.H. (2000) Crystal chemical aspects of vanadium: Polyhedral geometries, characteristic bond valences, and polymerization of (VO_n) polyhedral. Chemical Materials, 12(5), 1248–1259.

Shawe, D.R. (2011) Uranium-vanadium deposits of the Slick Rock district, Colorado. U.S. Geological Survey Professional Paper 576-F.

Sheldrick, G.M. (2015) Crystal structure refinement with SHELX. Acta Crystallographica, C71, 3–8.

MANUSCRIPT RECEIVED MARCH 3, 2019
MANUSCRIPT ACCEPTED AUGUST 14, 2019
MANUSCRIPT HANDLED BY FERNANDO COLOMBO

Endnote:

[1] Deposit item AM-19-127027, Supplemental table, CIF. Deposit items are free to all readers and found on the MSA website, via the specific issue's Table of Contents (go to http://www.minsocam.org/MSA/AmMin/TOC/2019/Dec2019_data/Dec2019_data.html).